

- mun.*, **63**, 831 (1987).
- Y. Dai, J. S. Swinnea, H. Steinfink, J. B. Goodenough and A. Campion, *J. Am. Chem. Soc.*, **109**, 5291 (1987).
  - Z. Iqbal, S. W. Steinhauser, A. Bose, N. Cipollini and H. Eckhardt, *Phys. Rev.*, **B36**, 2283 (1987).
  - S. K. Cho, D. Kim, J. S. Choi and K. H. Kim, *J. Phys. Chem. Solids*, **51**, 113 (1990).
  - H. Rosen, E. M. Engler, T. C. Strand, V. Y. Lee and D. Bethune, *Phys. Rev.*, **B36**, 726 (1987).
  - R. J. Hemley and H. K. Mao, *Phys. Rev. Lett.*, **58**, 2340 (1987).
  - A. K. Tyagi, S. J. Patwe, U. R. K. Rao and R. M. Iyer, *Solid State Commun.*, **65**, 1149 (1988).
  - S. R. Ovshinsky, R. T. Young, D. D. Allred, G. DeMaggio and G. A. Van der Leeden, *Phys. Rev. Lett.*, **58**, 2579 (1987).
  - R. N. Bhargava, S. P. Herko and W. N. Osborne, *Phys. Rev. Lett.*, **59**, 1468 (1987).
  - D. C. Harris, M. E. Hills and T. A. Hewston, *J. Chem. Ed.*, **64**, 847 (1987).
  - K. Takeshi, *Japan-U. S. Symposium on High Temperature Superconductivity*, pp. 13-8 (1987).

## Theoretical Studies on the A2 Hydrolysis of Methyl Acetimide<sup>1</sup>

Ikchoon Lee\*, Chang Kon Kim, and Bon-Su Lee

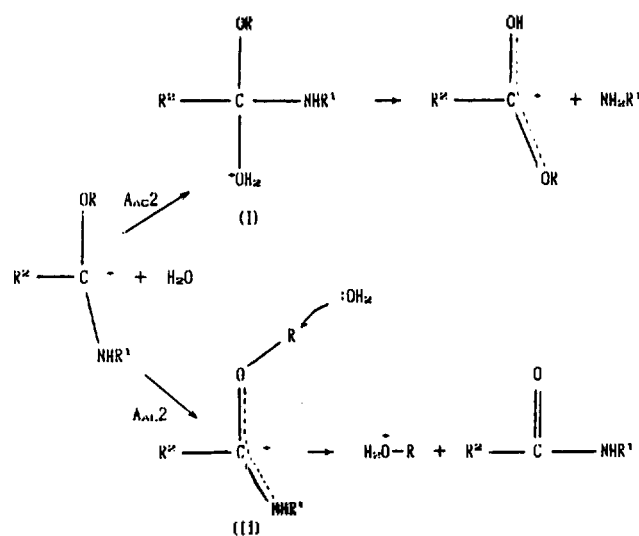
Department of Chemistry, Inha University, Incheon 402-751. Received November 13, 1989

Various mechanistic aspects of the A2 hydrolysis of methyl acetimide were explored using the MNDO method. As in the corresponding reactions of acetamide and methyl carbamate, a proton transfer pre-equilibrium exists between the N-protonated and the O-protonated tautomers, and the subsequent hydrolysis proceeds from the more stable N-protonated form. Of the two reaction pathways, the  $A_{AL}2$  path is favored in the gas phase and in concentrated acid solutions, whereas the  $A_{AC}2$  path is favored in less acidic solutions with a stable cationic tetrahedral intermediate formed in the rate determining step. Negative charge development on the alkoxy oxygen in the transition state suggested a rate increase with the increase in the electron withdrawing power of the alkoxy group. Calculations on the reaction processes with AM1 indicated that MNDO is more reliable in this type of work, although AM1 is better than MNDO in reproducing hydrogen bonds.

### Introduction

The interest in the solution phase studies on the acid hydrolysis of imidate ester<sup>2-7</sup> has long been centered around the reality of a tetrahedral addition intermediate<sup>2-14</sup> ((I) in Scheme 1) believed to participate in the  $A_{AC}2$  hydrolysis of carbonyl compounds<sup>15</sup> and its implications for the mechanism of ester aminolysis.<sup>16-18</sup> Unlike in the  $A_{AL}2$  hydrolysis of carbonyl compounds such as amides and carbamates, it is now well established that in the  $A_{AC}2$  hydrolysis of imidate esters the tetrahedral addition complex, (I), constitutes a key intermediate in the course of reaction. Moreover, it has been experimentally shown that two competing pathways are possible for the imidate hydrolysis in acid solution, giving either ester and amine products by an attack of water on the acyl carbon ( $A_{AC}2$  process) or amide and alcohol by an  $S_N2$  displacement of water at the alkoxy R ( $A_{AL}2$  process) of the N-protonated form of imidate esters (Scheme 1). The acid hydrolysis of 2,6-dimethylbenzimidate, which has a sterically hindered acyl carbon, has been shown to proceed predominantly (99%) by the  $A_{AL}2$  pathway,<sup>19</sup> while that of methylbenzimidate involves partial  $A_{AL}2$  process in relatively concentrated acid solution (18%  $A_{AL}2$  hydrolysis in 65%  $H_2SO_4$  solution).<sup>20</sup> Results of solution phase studies have also shown an enhancement of the hydrolysis rate with an increase in the electron withdrawing power of the alkoxy group of imidate esters.<sup>21</sup>

However we are not available the *ab initio* MO results and the gas-phase experimental data of the imidate hydrolysis or related works.

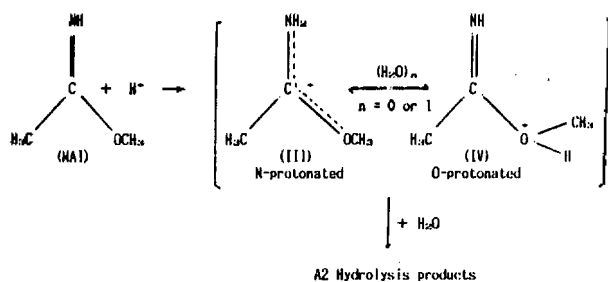


Scheme 1

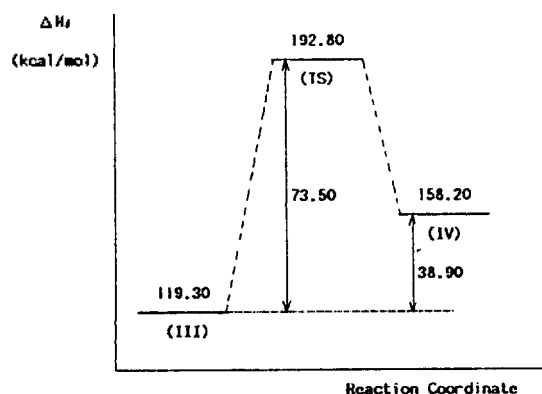
In this work, we investigated the acid hydrolysis of methyl acetimide MO theoretically using the MNDO and AM1 method<sup>22,23</sup> in order to explore various mechanistic possibilities and to elucidate substituent and solvent effects on the rate and mechanism of the imidate acid hydrolysis.

### Calculations

Standard MNDO program<sup>24</sup> was used throughout in this work. Geometrical parameters of all stationary point struc-



Scheme 2

Figure 1. Potential energy profile for the direct proton transfer, (III)  $\rightarrow$  (IV).

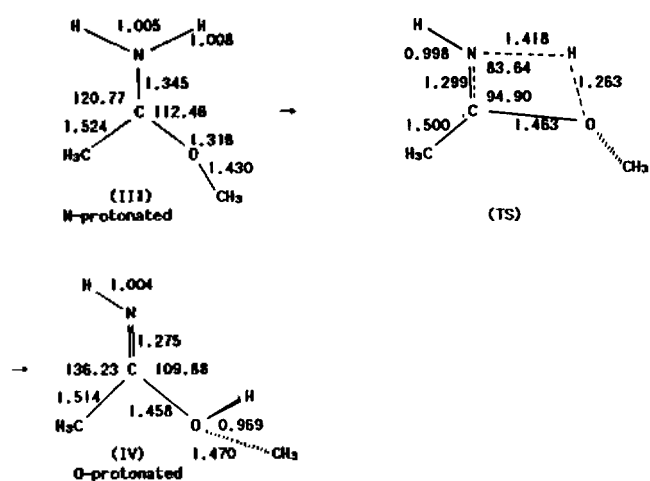
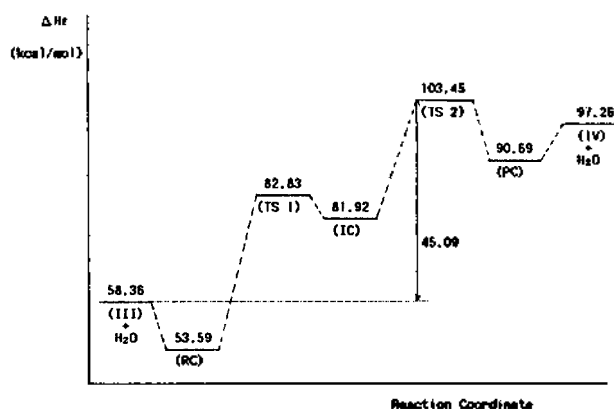
tures were fully optimized, and the transition states (TS) were located first using the reaction coordinate method<sup>25,26</sup> and then refined with the gradient norm minimization<sup>27,28</sup> to obtain their structures and energies. All the TSs were characterized by confirming only one negative eigenvalue in the Hessian matrix.<sup>29</sup> In the solvent effect studies, the geometries of TSs were fully optimized for the supermolecules consisting of substrate and attached solvate water molecules. Calculations were also carried out with AM1<sup>30</sup> in order to assess the influence of hydrogen bonds on solvent effect and reaction path.

## Results and Discussion

There are two basic sites, N and O, that can be protonated in methyl acetimidate as in acetamide and methyl carbamate, and either one of the two protonated tautomers can be a starting species in the A2 hydrolysis since imidates are known to be completely protonated even in a relatively weak acid solution.<sup>19,21</sup> We have therefore dealt with the proton transfer equilibrium between the two protonated tautomers (Scheme 2) involving no or one solvate water molecule before proceeding to the actual acid hydrolysis of methyl acetimidate.

### (I) Proton Transfer Equilibria

**(i) Direct Proton Transfer.** This corresponds to the  $n = 0$  case in Scheme 2, which is a direct intramolecular proton transfer process. Since the N-protonated form (III) is more stable by 38.91 kcal/mol than the O-protonated form (IV), the proton transfer from the major species (III) to the minor species (IV) is considered. This type of direct intramolecular proton transfer involves a typical 1,3-proton shift with a four-membered ring TS.<sup>31-33</sup> The activation barrier was relatively high (73.50 kcal/mol) so that such process may not be practicable, as it was also found to be the case in the in-

Figure 2. Geometries for the stationary point species on the potential energy profile for the direct proton transfer. (III)  $\rightarrow$  (IV) (bond lengths and angles are in Å and degree).Figure 3. Potential energy profile for the solvated proton transfer, (III) + H<sub>2</sub>O  $\rightarrow$  (IV) + H<sub>2</sub>O.

tramolecular proton transfers of acetamide and methyl carbamate.<sup>34,35</sup> The potential energy profile and the optimized geometries for the stationary point species are shown in Figures 1 and 2.

**(ii) Solvated Proton Transfer.** Here a proton is transferred through the intermediacy of one solvated water molecule ( $n = 1$  in Scheme 2), which acts as a proton-donor as well as an acceptor in a two-step intermolecular process; as a result a triple-well potential energy surface is obtained (Figure 3). There are two TSs in Figure 3. One is the deprotonation step (of (III)) by water, the other is the re-protonation step to form (IV) by H<sub>3</sub>O<sup>+</sup>. The optimized geometries of the stationary point species along the reaction coordinate are shown in Figure 4. The rate determining step in this process is the reprotonation step with the activation barrier of 45.09 kcal/mol, which is lower by 28.41 kcal/mol than that for the direct proton transfer. Although the overall proton transfer processes are very similar, the barrier is the highest for methyl acetimidate when a comparison is made with the MNDO barriers of the corresponding processes for acetamide (29.14 kcal/mol) and methyl carbamate (27.43 kcal/mol).<sup>34</sup>

### (II) A<sub>AC</sub>2 Hydrolysis

**(i) A<sub>AC</sub>2 Hydrolysis of N-protonated Tautomer.** The potential energy profile and the optimized geometries of sta-

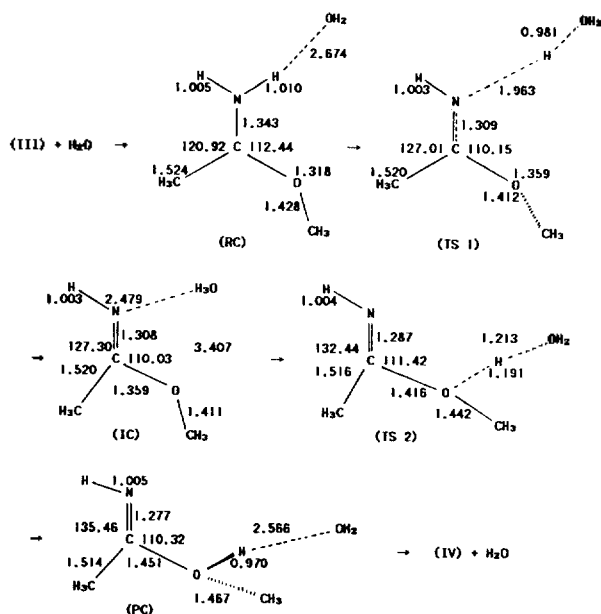


**Figure 4.** Geometries for the stationary point species on the potential energy profile for the solvated proton transfer. (III) + H<sub>2</sub>O → (IV) + H<sub>2</sub>O (bond lengths and angles are in Å and degree).

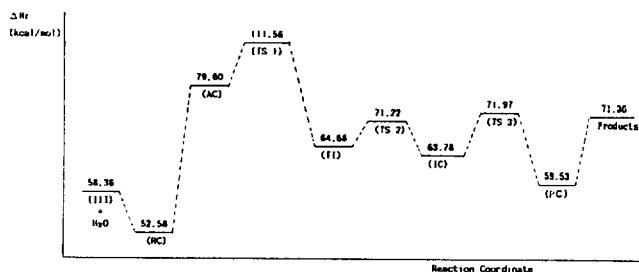


**Figure 5.** Potential energy profile for the AAC<sub>2</sub> hydrolysis of N-protonated tautomer, (III).

tionary point species involved in the AAC<sub>2</sub> type hydrolysis of the N-protonated tautomer, (III), are given in Figures 5 and 6. The overall process is quite similar to those involved in the A<sub>2</sub> hydrolysis of O-protonated tautomers of acetamide<sup>36</sup> and methyl carbamate.<sup>37</sup> The reactant complex(RC) is a π-type formed by nucleophile, water, approaching perpendicularly toward the molecular plane of the protonated substrate, (III). The RC then proceeds to form a transient addition complex (AC) by the nucleophilic attack of water molecule at the acyl carbon. The AC is made up of an oxonium ion form, which is similar to the one proposed by McClelland<sup>19</sup> based on his solution phase studies; this is however not a stable equilibrium species but corresponds to a mere stationary point on the potential energy surface (Figure 5) preceding the rate determining step. In the rate determining step a proton is transferred to the N atom, which is then followed by a stable tetrahedral intermediate(TI). This TI is a cationic equilibrium species which has been proposed to participate in the AAC<sub>2</sub> hydrolysis of imidate esters by Okuyama *et al.*<sup>38</sup> Thus our MNDO results are in complete agreement with the experimentally postulated mechanism, in which a stable cationic tetrahedral intermediate is formed by a rate determining attack of water on the acyl carbon.

The proton can be transferred to the methoxy-O atom in-

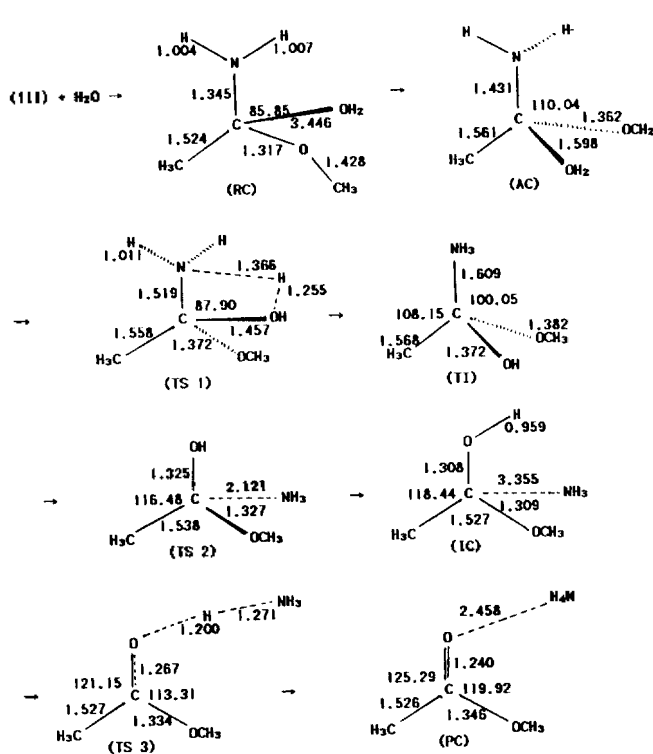


**Figure 6.** Geometries for the stationary point species on the potential energy profile for the AAC<sub>2</sub> hydrolysis of N-protonated tautomer. (III) + H<sub>2</sub>O → CH<sub>3</sub>CO<sub>2</sub>CH<sub>3</sub> + NH<sub>4</sub><sup>+</sup> (bond lengths and angles are in Å and degree).

stead of the N atom in the AC, in which case the hydrolysis products will be either acetamide and protonated methanol or iso-acetamide and protonated methanol. These pathways, however, involve a higher activation energy barrier by 13.58 kcal/mol compared to the process through the N-protonated form giving methyl acetate and ammonium ion as products; this is again in agreement with the experimental facts that the AAC<sub>2</sub> hydrolysis products of imidate esters are normally esters and ammonium ions.<sup>2-7</sup>

The alternative pathway through the methoxy-O protonated form after the AC is hence unfavorable due to the higher activation barrier than the principal pathway through the N-protonated form, as evidenced by the absence of products originating from such alternative process.

We have nevertheless elaborated upon the mechanism of this alternative process. The rate determining step in this path is also a proton transfer to the methoxy-O in the AC, which is followed by intermediate complex(IC) formation; the IC is not a tetrahedral type but is similar to the RC, a π-type complex formed by the leaving methanol molecule oriented perpendicularly to the molecular plane of O-protonated acetamide. The leaving group, methanol, in the IC can abstract a proton either from the carbonyl oxygen giving acetamide or from the N atom giving iso-acetamide. Iso-acetamide is known to tautomerize to a more stable tautomer, acetamide.<sup>39, 40</sup> according to our MNDO results, the activation energy for iso-acetamide formation is higher by 2.32 kcal/mol than that for acetamide formation and, furthermore, acetamide is more stable by 3.20 kcal/mol than iso-acetamide. The formation of acetamide is therefore preferred both kinetically and thermodynamically. The potential energy

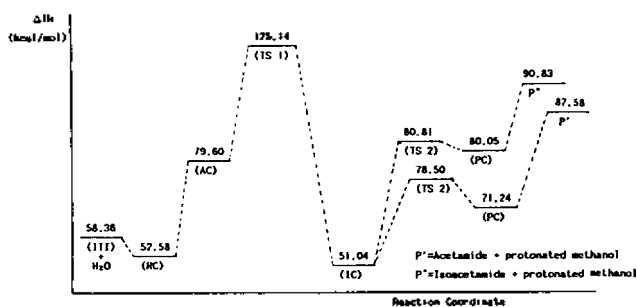


Figure 7. Potential energy profile for the  $A_{AC2}$  hydrolysis N-protonated tautomer, (III).

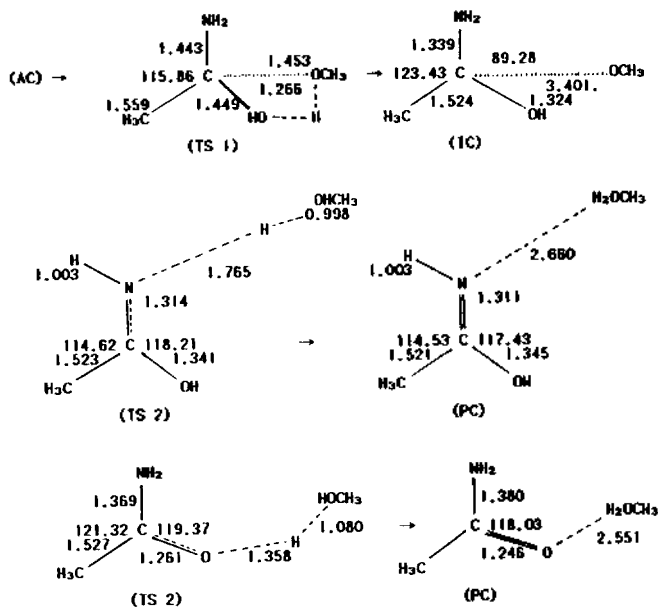


Figure 8. Geometries for the stationary point species on the potential energy profile for the  $A_{AC2}$  hydrolysis of N-protonated tautomer, (III) +  $H_2O \rightarrow$  Isoacetamide + protonated methanol or Acetamide + protonated methanol (bond lengths and angles are in Å and degree).

profiles and the optimized stationary point structures are shown in Figures 7 and 8.

(ii)  $A_{AC2}$  hydrolysis of Methoxy-O Protonated Tautomer.

We will now consider the  $A_{AC2}$  hydrolysis of the methoxy-O protonated tautomer, (IV), which is formed in the pre-equilibrium with the N-protonated form, (III), (Scheme 2). Our MNDO results show that the reaction proceeds through a typical triple-well potential energy surface with three wells corresponding to reactant (RC), intermediate (IC) and product (PC) complexes. The potential energy profile and the optimized stationary point structures are presented in Figures 9 and 10. Inspection of Figure 10 reveals that the RC and IC have structures similar to those of the corresponding complexes of the N-protonated tautomer, with only difference of the leaving group,  $NH_3$  in this case, instead of methanol. In the rate determining step following the RC, the nucleophile, water, attacks the acyl carbon with concerted formation of bond  $C \cdots OH_2$  and breaking of the leaving group, methanol. This  $S_N2$  type direct substitution is then followed by a fast product formation step, in which a proton is abstracted from water by the leaving methanol molecule giving iso-

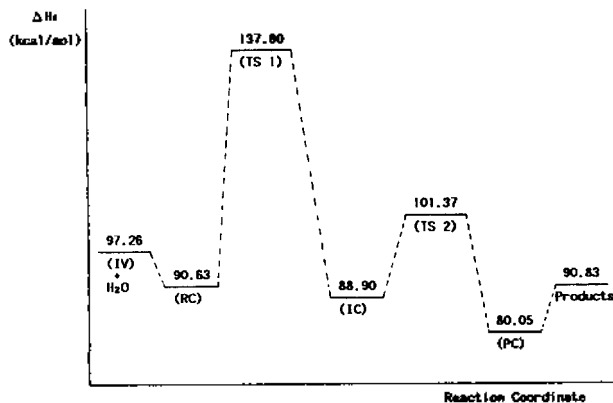


Figure 9. Potential energy profile for the  $A_{AC2}$  hydrolysis of Methoxy O-protonated tautomer.

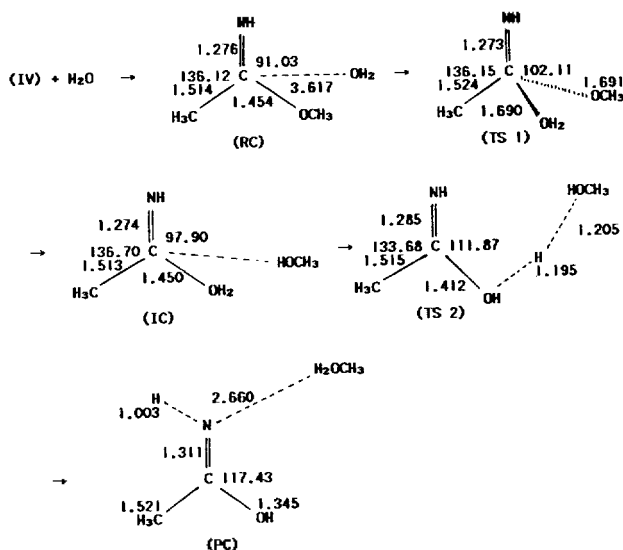
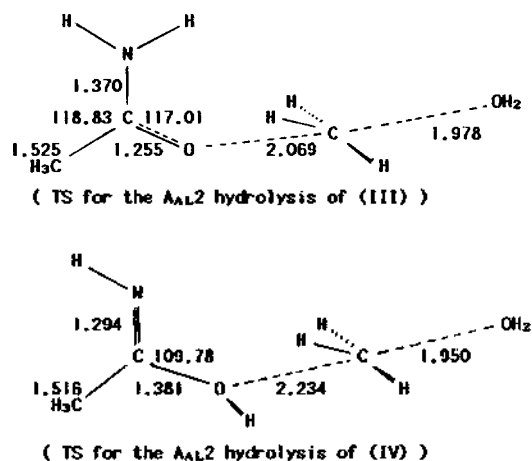


Figure 10. Geometries for the stationary point species on the potential energy profile for the  $A_{AC2}$  hydrolysis of Methoxy O-protonated tautomer, (IV) +  $H_2O \rightarrow$  Isoacetamide + protonated methanol (bond lengths and angles are in Å and degree).

tamide and protonated methanol.

This pathway through the O-protonated tautomer is however unfavorable comparing to that through the N-protonated form both kinetically (higher activation energy by 26.24 kcal/mol) and thermodynamically (products are less stable by 19.47 kcal/mol). We can therefore conclude that the principal pathway in the  $A_{AC2}$  hydrolysis of methyl acetimidate is through the more stable N-protonated tautomer, which is in agreement with the solution phase experimental results.<sup>2-7</sup> This  $A_{AC2}$  hydrolysis mechanism for methyl acetimidate is, however, in contrast to that for acetamide and methyl carbamate in which the  $A_{AC2}$  hydrolysis proceeds through a more unstable protonated tautomer (N-protonated).<sup>36, 37</sup> An origin of this discrepancy in the reaction path may well be a relatively large difference in stabilities of the two protonated tautomers for methyl acetimidate ( $\Delta \Delta H_f = 38.90$  kcal/mol) compared to the corresponding differences for acetamide ( $\Delta \Delta H_f = 17.19$  kcal/mol)<sup>36</sup> and methyl carbamate ( $\Delta \Delta H_f = 18.95$  kcal/mol).<sup>37</sup> In this connection, it is interesting to note that in the  $A_{AC2}$  hydrolysis of methyl carbamate the reaction



**Figure 11.** TS geometries for the  $A_{AL}2$  hydrolysis of (III) and (IV) (bond lengths and angles are in Å and degree).

pathway through the most unstable protonated tautomer, methoxy-O-protonated ( $\Delta \Delta H_f = 36.12$  kcal/mol compared to the most stable carbonyl-O-protonated form), has also been found to be unfavorable both kinetically and thermodynamically.

### (III) $A_{AL}2$ Hydrolysis

An  $S_N2$  displacement analogous to the  $A_{AL}2$  hydrolysis of carboxylate ester (Scheme 1) has been reported to take place predominantly in the acid hydrolysis of 2,6-dimethylbenzimidate esters in which the acyl carbon is sterically hindered,<sup>19</sup> and partially in the hydrolysis of unhindered methyl benzimidate in highly acidic solution (ca. 18% in 65%  $H_2SO_4$  solution).<sup>20</sup>

The MNDO results on this reaction mode show that the reaction proceeds through a simple double-well potential energy surface with two wells corresponding to RC and PC, which are the same complexes found in the  $A_{AC}2$  hydrolysis of the N-protonated tautomer above. The O-protonated tautomer, (IV), also proceeds by the double-well potential energy surface with the RC and PC found in the corresponding  $A_{AC}2$  hydrolysis.

The TS in between the two wells has a typical  $S_N2$  TS structure (Figure 11) with the heat of formation of 107.19 kcal/mol for the reaction pathway through N-protonated (III) and 119.23 kcal/mol for the pathway through O-protonated (IV). The former is lower by 4.37 kcal/mol than the barrier found in the  $A_{AC}2$  hydrolysis through the same N-protonated tautomer, indicating that the  $A_{AC}2$  process is preferred to the  $A_{AL}2$  pathway under solvent free condition. Since the acyl carbon of methyl acetimidate is not sterically hindered, this may seem rather surprising. However this preference of the  $A_{AL}2$  path to the  $A_{AC}2$  process when there is no (or not enough) solvate molecules can be readily accommodated by the experimental observations of a decrease in the rate ratio of  $k_{AC}2/k_{AL}2$  with the increase in the acidity of solution,<sup>19,20</sup> since the TS leading to the acyl addition ( $A_{AC}2$ ) is more salted-out by increasing acidity than the TS leading to alkyl substitution ( $A_{AL}2$ ). This means that the present MNDO results with no solvated water molecules are completely in line with the experimental observation in strong acid solutions predicting a preference of the  $A_{AL}2$  to the  $A_{AC}2$  path.

**Table 1.** Solvation Effects on the TSs of the  $A_{AC}2$  and  $A_{AL}2$  Paths

$n^a$	$A_{AC}2$	$A_{AL}2$	$\Delta \Delta H_f^c$
0	111.56 <sup>b</sup>	107.23	4.33
1	44.72	41.61	3.11
2	-20.98	-23.62	2.64
3	-86.95	-87.88	0.93
4	-152.07	-151.63	-0.44

<sup>a</sup>Number of solvate water molecule. <sup>b</sup>Heat of formation of TS:  $\Delta H_f$  (TS) in kcal/mol. <sup>c</sup> $\Delta \Delta H_f = \Delta H_f(A_{AC}2) - \Delta H_f(A_{AL}2)$ .

In order to study the effect to solvation, we have attached four water molecules to the TSs involved in the two pathways, i.e.,  $A_{AC}2$  and  $A_{AL}2$  paths. The results are summarized in Table 1. To our surprise, only four solvated water molecules in the TS were enough to reverse the trend in the activation barrier in favor of the  $A_{AC}2$  process, indicating correctly that in the relatively dilute acid the  $A_{AC}2$  process will become dominant. We are aware of the inherent weakness in MNDO of not properly accounting for hydrogen bond energy,<sup>30</sup> especially in a work involving solvent effect, but here we are primarily interested in the relative energy barriers of two reaction paths for which the discrepancies due to the improper account of hydrogen bond in the TSs may cancel out<sup>31</sup>; we may then expect that the difference in the extent of charge-dipole interaction between substrate and attached solvent molecules predominates over the solvent effect (vide infra). The reversal of relative barrier heights in favor of the  $A_{AC}2$  path with only four solvate water molecules will become even more real in the bulk solvent system. Thus in dilute acid solution, the  $A_{AC}2$  path will be extremely favorable as experimentally found.

In order to assess the influence of hydrogen bonds on the solvent effect and reaction path, we carried out similar computations on the reaction processes with AM1, since AM1 is known to reproduce hydrogen bonds in a reasonably satisfactory manner.<sup>32</sup> We found essentially the same trends as those found using MNDO with somewhat lower activation barriers, but there was a conspicuous difference between the two methods: no optimized structure for the O-protonated tautomer, (IV), is obtainable by AM1, but instead a long-range complex, (V), involving partial cleavage of the C-O bond is found. We therefore proceeded further to check the reality of the O-protonated tautomer by carrying out *ab initio* calculations at the 3-12G level,<sup>41</sup> and found that the structure (IV) does indeed exist as the MNDO results predicted. Thus it appears that MNDO is more reliable than AM1 for this type of work correctly reproducing *ab initio* trends.

An overview of activation barriers studied in this work is presented in Figure 12. Admittedly the MNDO barrier heights shown in Figure 12 are in general considerably higher than the experimental solution phase values.<sup>42</sup> This is due to

<sup>31</sup>In a previous work involving proton transfer equilibria in aqueous system, it has been shown that MNDO and AM1 show exactly the same trends with only difference of AM1 having somewhat lower activation barriers. We have concluded there that MNDO is just as useful for such type of work in which we are primarily interested in the relative barrier heights between competing reaction paths. I. Lee, C. K. Kim, B-S Lee and S. C. Kim, *Tetrahedron*, **44**, 7345 (1988).

<sup>32</sup>The results are presented as Supplementary Materials.

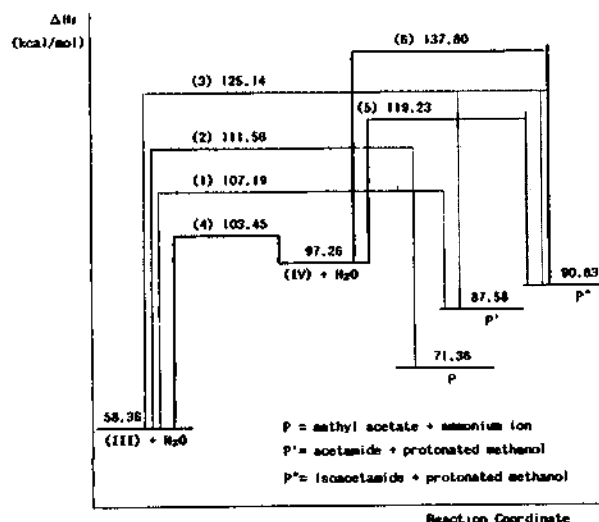
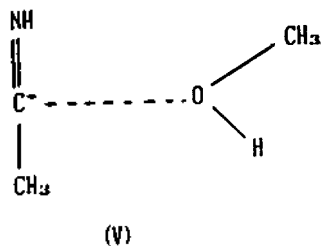


**Figure 12.** An overview of activation barriers involving in the A2 hydrolysis of methyl acetimidate. Dotted lines A2 hydrolysis process of (III). (1) is an  $A_{AI,2}$  path, and (2) and (3) are  $A_{AC,2}$  paths. Solid lines are A2 hydrolysis processes of (IV). (4) is a solvated proton transfer process, (5) is an  $A_{AI,2}$  path and (6) is an  $A_{AC,2}$  path.

**Table 2.** Charges (Electronic Charge Unit) of Heavy Atoms for the Relevant Species on the  $A_{AC,2}$  Hydrolysis Path of N-protonated Tautomer

	C <sub>1</sub> <sup>a</sup>	C <sub>2</sub>	C <sub>3</sub>	N	O
(III)	+0.4162	+0.2121	-0.0028	-0.2392	-0.2593
(AC)	+0.4348	+0.2122	-0.0007	-0.3633	-0.3552
(TS I)	+0.3559	+0.2176	+0.0101	-0.2588	-0.3736

<sup>a</sup>C<sub>1</sub>, C<sub>2</sub> and C<sub>3</sub> are the acyl carbon, methoxy methyl and methyl carbon, respectively.



the well known weakness of overestimating the barrier heights by the MNDO method.<sup>30,43</sup> Even though the absolute values of barrier heights may be unrealistic, the relative values have been useful in the elucidation of mechanistic features.<sup>44-50</sup>

#### (IV) Effects of Substituent on Alkoxy Oxygen

Pletcher *et al.*<sup>21</sup> has reported the Taft  $\rho^*$  coefficient of +2.1 for alkoxy oxygen in the  $A_{AC,2}$  hydrolysis of N-methyl acetimidate esters, and the rate of the  $A_{AC,2}$  hydrolysis of imidate esters has been shown to increase with the electron withdrawing power of the group R of the alkoxy group in the order,  $\text{CH}_3\text{CH}_2 < \text{CH}_3\text{OCH}_2\text{CH}_2 < \text{CF}_3\text{CH}_2$ .

We have shown in Table 2 charges of heavy atoms in the optimized structures of the ground state (III), the transient addition complex(AC) and the TS. Reference to this Table 2 reveals that the negative charge on the alkoxy oxygen in-

creases gradually as the reaction proceeds until the TS is reached, suggesting that an electron withdrawing group R on the alkoxy oxygen will delocalize the developing negative charge and will stabilize the TS and hence will increase the rate. Thus the experimental rate enhancement found by Pletcher *et al.* can be nicely accounted for.

## Conclusions

The major conclusions in this MNDO investigation of the acid hydrolysis of methyl acetimidate can be summarized as follows:

(i) The stability of the N-protonated tautomer is substantially greater than that of the O-protonated form, so that the hydrolysis proceeds largely through the more stable N-protonated form.

(ii) The acyl addition pathway ( $A_{AC,2}$ ) proceeds *via* a transient addition complex(AC) and a stable cationic tetrahedral intermediate(TI).

(iii) In the non- or less-solvating concentrated acid solution, the alkyl substitution pathway ( $A_{AI,2}$ ) is favored, whereas in the low acid solution the acyl addition path ( $A_{AC,2}$ ) becomes dominant.

(iv) Negative charge development on the alkoxy oxygen in the TS of the  $A_{AC,2}$  hydrolysis suggested an increase in the rate with the increase in the electron withdrawing power of the alkoxy group.

**Acknowledgements.** We thank the Ministry of Education and the Korea Science Engineering Foundation for support of this work. This research has been performed using the SEC computer system of the joint project between SEC and IBM Korea.

## References

1. Part 63 of the series: Determination of Reactivity by MO theory.
2. V. F. Smith, Jr., and G. L. Schmir, *J. Am. Chem. Soc.*, **97**, 3171 (1975).
3. R. K. Chaturvedi and G. L. Schmir, *ibid.*, **90**, 4413 (1968).
4. B. A. Cunningham and G. L. Schmir, *ibid.*, **89**, 917 (1967).
5. T. Okuyama and G. L. Schmir, *ibid.*, **94**, 8805 (1972).
6. A. C. Satterthwait and W. P. Jencks, *ibid.*, **96**, 7031 (1974).
7. R. H. Dewolfe and F. B. Augustine, *J. Org. Chem.*, **30**, 669 (1965).
8. M. L. Bender, *Chem. Rev.*, **60**, 53 (1960).
9. S. L. Johnson, *Adv. Phys. Org.*, **5**, 237 (1967).
10. H. B. Burgi, J. D. Dunitz and E. Shaffer, *J. Am. Chem. Soc.*, **95**, 5064 (1973).
11. H. B. Burgi, J. M. Lehn and G. Wipff, *ibid.*, **96**, 1956 (1974).
12. S. Scheimer, W. N. Lipscomb and D. A. Kleier, *ibid.*, **98**, 4770 (1976).
13. S. J. Weiner, U. C. Singh and P. A. Kollman, *ibid.*, **107**, 2219 (1985).
14. S. Yamabe and T. Minato, *J. Org. Chem.*, **48**, 2972 (1983).
15. J. March, "Advanced Organic Chemistry", 3rd Ed., John

- Wiley and Sons, New York, 1985, p.334.
16. G. M. Blackburn and W. P. Jencks, *J. Am. Chem. Soc.*, **90**, 2638 (1968).
  17. A. C. Satterthwait and W. P. Jencks, *ibid.*, **96**, 7018 (1974).
  18. G. L. Schmir and B. A. Cunningham, *ibid.*, **87**, 5692 (1965).
  19. R. A. McClelland, *ibid.*, **97**, 3177 (1975).
  20. C. R. Smith and K. Yates, *ibid.*, **94**, 8811 (1972).
  21. T. C. Pletcher, S. Koehler and E. H. Cords, *ibid.*, **90**, 7072 (1968).
  22. M. J. S. Dewar and W. Thiel, *ibid.*, **99**, 4899 (1977).
  23. M. J. S. Dewar and H. S. Rzepa, *ibid.*, **100**, 784 (1978).
  24. Available from Quantum Chemistry Program Exchange (QCPE), No. 506.
  25. K. Muller, *Angew. Chem., Int. Ed.*, **19**, 1 (1980).
  26. S. Bell and J. S. Crighton, *J. Chem. Phys.*, **80**, 2464 (1984).
  27. A. Kormonichi, K. Ishida and K. Morokuma, *Chem. Phys. Lett.*, **45**, 595 (1977).
  28. J. W. McIver, Jr., and A. Kormonichi, *J. Am. Chem. Soc.*, **94**, 2025 (1972).
  29. I. G. Csizmadia, 'Theory and Practice of MO calculations on Organic Molecules', Elsevier, Amsterdam, 1976, p. 237.
  30. M. J. S. Dewar, E. G. Zoebisch, E. F. Healy and J. J. P. Stewart, *J. Am. Chem. Soc.*, **107**, 3902 (1985).
  31. F. M. Menger, J. Grossman and D. C. Liotta, *J. Org. Chem.*, **48**, 905 (1983).
  32. K. Yamashita, M. Kaminoyama, T. Yamabe and K. Fukui, *Theoret. Chim. Acta*, **60**, 303 (1981).
  33. I. Lee, J. K. Cho and B-S. Lee, *J. Comput. Chem.*, **5**, 217 (1984).
  34. I. Lee, C. K. Kim and H. S. Seo, *Bull. Korean Chem. Soc.*, **7**, 395 (1986).
  35. I. Lee, C. K. Kim, B-S. Lee and S. C. Kim, *Tetrahedron*, **44**, 7345 (1988).
  36. I. Lee, C. K. Kim and H. S. Seo, *Tetrahedron*, **42**, 6677 (1986).
  37. I. Lee, C. K. Kim and B. C. Lee, *J. Comput. Chem.*, **8**, 794 (1987).
  38. T. Okuyama, T. C. Pletcher, D. J. Sahn and G. L. Schmir, *J. Am. Chem. Soc.*, **95**, 1253 (1973).
  39. J. March, 'Advanced Organic Chemistry', 3rd Ed., John Wiley and Sons, New York, 1970, p. 788.
  40. A. L. J. Beckwith in 'The Chemistry of Amides', J. Zabicky, Ed., Interscience, New York, 1970, pp. 110-125.
  41. W. J. Hehre, L. Radom, P. V. R. Schleyer and J. A. Pople, 'Ab Initio Molecular Orbital Theory', John Wiley and Sons, New York, 1986, pp. 76-79.
  42. Activation enthalpy for the  $A_{Ac}2$  hydrolysis of methyl benzimidate in 0.12 N-HClO<sub>4</sub> solution has been reported to be 18.8 kcal/mol<sup>7</sup> and the  $A_{Ac}2$  hydrolysis of methyl 2,6-dimethylbenzimidate in 30.41%-H<sub>2</sub>SO<sub>4</sub> solution has been reported to be 25.4 kcal/mol.<sup>19</sup>
  43. W. Thiel, *J. Am. Chem. Soc.*, **103**, 1420 (1981).
  44. M. J. S. Dewar and M. L. McKee, *ibid.*, **100**, 7499 (1978).
  45. M. J. S. Dewar, D. J. Nelson, P. B. Shevlin and K. A. Biesiada, *ibid.*, **103**, 2802 (1981).
  46. M. J. S. Dewar and L. Chantranupong, *ibid.*, **105**, 7152 (1983).
  47. M. J. S. Dewar and L. Chantranupong, *ibid.*, **105**, 7161 (1983).
  48. F. Carrion and M. J. S. Dewar, *ibid.*, **106**, 3531 (1984).
  49. M. J. S. Dewar and D. R. Kuhn, *ibid.*, **106**, 5256 (1984).
  50. M. J. S. Dewar and K. M. Merz, Jr., *ibid.*, **107**, 6111 (1985).

## Determination of Ag(I) at a Chemically Modified Electrode Based on 2-Imino-cyclopentane-dithiocarboxylic Acid

Jeong-Sik Yeom, Mi-Sook Won, Sung-Nak Choi, and Yoon-Bo Shim\*

*Department of Chemistry, College of Natural Science, Pusan National University, Pusan 609-390*

*Received December 5, 1989*

Chemically modified electrodes (CMEs), based on 2-imino-1-cyclopentane-dithiocarboxylic acid (icdc) containing carbon paste, have been characterized using cyclic voltammetric techniques. Ag(I) was chemically deposited on the CMEs, and voltammograms were obtained with the electrode in a separate buffer solution. The CME surface can be regenerated with exposure to acid and reused for deposition. In 10 deposition/measurement/regenerate cycles, the linear response has been reproduced up to  $1 \times 10^{-6}$  M in linear sweep voltammetry and  $1 \times 10^{-8}$  M in differential pulse voltammetry with relative standard deviation of 5.2% and 12.4%, respectively. The sensitivity increased with deposition time and scanning rate, and detection limit was  $1 \times 10^{-7}$  M and  $1 \times 10^{-9}$  M at 20 minutes deposition in the linear sweep voltammetry and differential pulse voltammetry, respectively. The presence of some metal ions does not influence the silver ion response. Satisfactory results were obtained for the analysis of the silver ion for a variety of reference materials without interference of Hg ion at the condition of pH = 5-6.

### Introduction

Until now stripping voltammetry have been recognized as

one of the most sensitive electrochemical methods for the determination of trace metals. This utilizes both of the trace organic and inorganic analysis. In general, this method is